Table 1 Correlation among hypomethylation of individual repetitive elements, CT antigens, and hypermethylation of promoter CpG islands

	Alu	LINE1	*NY-ESO-1*	*MAGE-C1*	*HOXA9*	*NEFH*	*UCHL1*	*MT1M*
Background mucosae								
Alu	–	0.063	0.152	−0.132	**−0.351**	**−0.240**	**−0.231**	**−0.398**
LINE1		–	0.095	0.092	**−0.313**	**−0.464**	**−0.441**	**−0.554**
NY-ESO-1			–	0.038	**−0.356**	−0.024	0.010	**−0.238**
MAGE-C1				–	−0.088	−0.002	0.008	0.037
HOXA9					–	**0.341**	**0.632**	**0.490**
NEFH						–	**0.561**	**0.544**
UCHL1							–	**0.312**
MT1M								–
ESCC								
Alu	–	**0.502**	**0.307**	**0.240**	−0.162	0.093	−0.002	0.181
LINE1		–	**0.470**	**0.383**	**−0.386**	0.189	−0.049	**−0.262**
NY-ESO-1			–	**0.566**	−0.182	**0.240**	0.139	−0.019
MAGE-C1				–	**−0.268**	0.171	0.060	0.082
HOXA9					–	0.057	0.133	0.178
NEFH						–	**0.268**	−0.085
UCHL1							–	**0.381**
MT1M								–

Coefficient values shown in bold type denote that p value is <0.05

Table 2 Association between hypomethylation and exposure to risk factors

Sample	*N*	Alu		LINE1		*NY-ESO-1*		*MAGE-C1*	
		Mean ± SD	p value	Mean ± SD	p value	Mean ± SD	p value	Mean ± SD	p value
Normal mucosae									
Smoking history									
(−)	53	46.3 ± 2.2	0.411	79.0 ± 3.6	0.054	99.8 ± 0.4	0.474	99.5 ± 2.9	0.316
(+)	42	46.7 ± 2.6		80.6 ± 4.2		99.6 ± 1.3		99.9 ± 0.2	
Alcohol history									
(−)	61	46.5 ± 2.3	0.837	79.5 ± 3.8	0.517	99.8 ± 0.2	0.096	99.9 ± 0.2	0.337
(+)	34	46.4 ± 2.6		80.1 ± 4.1		99.4 ± 1.4		99.3 ± 3.6	
Background mucosae									
Smoking history									
(−)	15	45.1 ± 2.2	0.324	79.5 ± 4.9	0.650	99.5 ± 0.9	0.786	99.9 ± 0.2	0.683
(+)	74	45.8 ± 2.3		78.7 ± 7.0		99.6 ± 1.5		99.8 ± 0.7	
Alcohol history									
(−)	11	45.6 ± 1.0	0.866	79.8 ± 5.6	0.613	99.5 ± 1.1	0.828	99.9 ± 0.2	0.623
(+)	78	45.7 ± 2.4		78.7 ± 6.8		99.6 ± 1.4		99.8 ± 0.7	
ESCC									
Smoking history									
(−)	17	42.7 ± 3.1	0.433	61.3 ± 13.0	0.734	77.4 ± 34.1	0.106	86.6 ± 26.4	0.184
(+)	76	41.9 ± 3.9		62.4 ± 11.9		91.9 ± 18.1		95.7 ± 10.4	
Alcohol history									
(−)	12	41.7 ± 3.6	0.746	61.4 ± 15.9	0.810	85.1 ± 33.6	0.495	85.8 ± 30.8	0.316
(+)	81	42.1 ± 3.8		62.3 ± 11.5		89.9 ± 20.4		95.2 ± 10.6	

Table 3 Association between hypomethylation and clinicopathological findings

Variable	*N*	Alu		LINE1		*NY-ESO-1*		*MAGE-C1*	
		Mean ± SD	*p* value	Mean ± SD	*p* value	Mean ± SD	*p* value	Mean ± SD	*p* value
Depth of tumor									
T1/T2	9	40.2 ± 3.0	0.146	64.9 ± 8.6	0.399	89.3 ± 20.7	0.894	95.2 ± 5.9	0.737
T3/T4	66	42.1 ± 3.6		61.2 ± 12.5		90.3 ± 21.6		93.3 ± 17.2	
Tumor differentiation									
Poorly	12	41.2 ± 5.0	0.463	60.1 ± 14.7	0.932	92.1 ± 16.6	0.665	98.0 ± 3.2	0.288
Moderately/Well	33	42.3 ± 4.0		60.5 ± 10.8		88.9 ± 23.1		91.7 ± 20.0	
Lymph node metastasis									
Negative	11	40.7 ± 3.4	0.208	60.6 ± 8.8	0.715	95.7 ± 12.7	0.369	97.5 ± 3.5	0.392
Positive	65	42.1 ± 3.6		62.0 ± 12.6		89.4 ± 22.3		92.9 ± 17.3	
Multiplicity of tumor									
Solitary	74	41.8 ± 3.9	0.641	61.6 ± 12.3	0.251	87.3 ± 24.5	0.240	93.0 ± 16.5	0.310
Multiple	8	42.5 ± 3.8		62.0 ± 11.0		97.6 ± 5.6		99.0 ± 1.3	
Tumor recurrence									
Negative	79	41.8 ± 3.7	0.460	62.5 ± 12.5	0.373	89.3 ± 22.2	0.609	93.4 ± 16.0	0.393
Positive	9	42.8 ± 3.8		58.6 ± 10.7		93.2 ± 16.5		98.0 ± 3.3	

Table 4 Association between hypomethylation and expression of CT antigen genes

Sample ID.	*NY-ESO-1*		*MAGE-C1*	
	Methylation level (%)	Immunohistochemistry	Methylation level (%)	Immunohistochemistry
Background mucosae				
ES-29	93.3	−	100.0	−
ES-39	87.9	−	99.1	−
ES-49	99.8	−	99.9	−
ES-58	97.5	−	93.7	−
ES-59	100.0	−[a]	99.8	−[b]
ES-62	100.0	−	100.0	−
ESCC				
ES-29	12.2	+[a] (diffuse)	72.1	−
ES-39	80.3	−	92.7	−
ES-49	51.0	−	51.9	+[b] (hetero)
ES-58	53.1	+[a] (hetero)	54.0	+ (hetero)
ES-59	99.7	−[a]	93.7	+ (hetero)
ES-62	99.4	−	97.4	−[b]

[a] Microscopic findings are shown in Fig. 2

[b] Microscopic findings are shown in Supplementary Fig. 3

background mucosa with demethylation. There was no specimen that stained positive without demethylation, supporting the role of methylation status in expression regulation of the CT antigen genes.

Discussion

In this study, we demonstrated that hypomethylation of Alu and LINE1 was present in ESCCs. Although the presence of global hypomethylation is considered to be a universal phenomenon across various types of cancers [14, 29–31], this is the first report on its presence in ESCCs and provides a fundamental piece of information. Also, it was striking that hypomethylation of Alu, but not LINE1, was present in non-cancerous background mucosae of ESCC patients. This strongly indicated that Alu hypomethylation is induced earlier than LINE1 hypomethylation during carcinogenesis of ESCCs. The Alu hypomethylation was considered to be involved in the epigenetic field for cancerization, and might have potential as an epigenetic marker for ESCC risk estimation.

In the background mucosae, hypomethylation of repetitive elements negatively correlated with hypermethylation of promoter CpG islands of the four genes, *HOXA9*, *NEFH*, *UCHL1*, and *MT1M*. This finding suggested a possibility

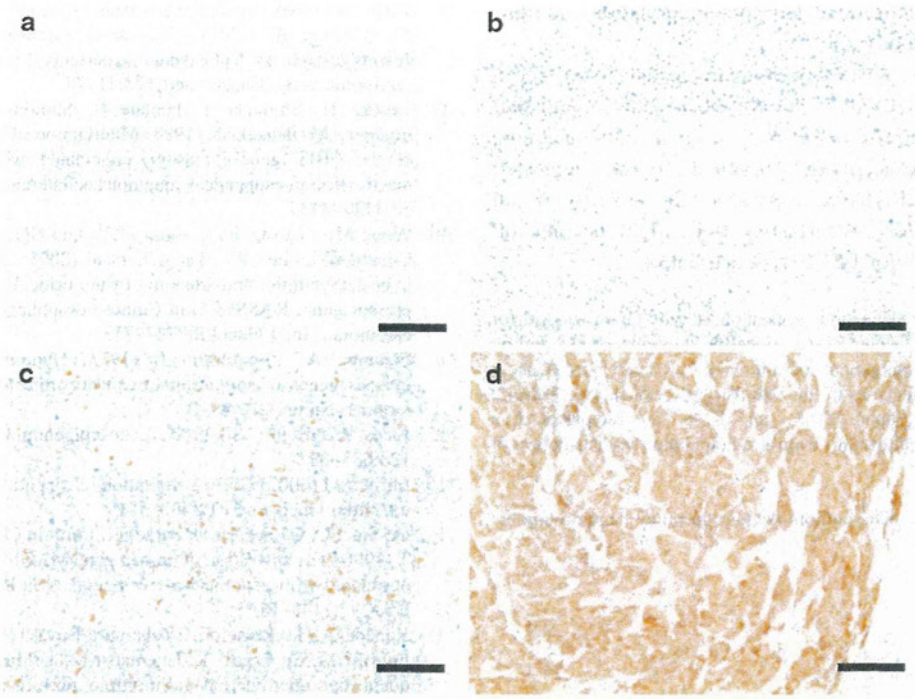

Fig. 2 Representative immunohistochemical staining of NY-ESO-1 in surgical specimens. **a** Non-cancerous background mucosa (ES-59, methylation level = 100.0%), **b** ESCC with full methylation (ES-59, methylation level = 99.7%), **c** ESCC with partial demethylation (ES-58, methylation level = 53.1%), and **d** ESCC with almost complete demethylation (ES-29, methylation level = 12.2%) are presented. A *scale bar* represents 100 μm. Neither the background specimen nor the specimen of ESCC with full methylation had staining. Heterogeneous staining, mainly nuclear, was observed in the specimen with partial demethylation. Diffuse staining in both cytoplasm and nucleus was observed in the specimen with almost complete demethylation. The result of immunohistochemistry was consistent with methylation status of CT antigen genes

that global hypomethylation and hypermethylation of some promoter CpG islands were caused by shared factors. In our study, however, while hypermethylation of these four genes is known to correlate with smoking history [8, 9], no association was found between hypomethylation and exposure to risk factors, including history of cigarette smoking and alcohol intake. It was considered that cigarette smoking and alcohol intake were more closely associated with hypermethylation of these CpG islands than with global hypomethylation.

In the stomach, we previously showed that hypomethylation of Alu, LINE1, and Satα is present and that Alu hypomethylation was more sensitive to hypomethylation due to *Helicobacter pylori* infection than the other repetitive elements [28]. Taken together, Alu seems to be most susceptible to hypomethylation due to exposure to carcinogenic stimuli. The different susceptibility to hypomethylation between Alu and LINE1 might be attributed to the differences in their intrinsic functions. Alu depends on the proteins encoded by LINE1 for its retrotranscription and transposition [32], whereas LINE1 is transposable autonomously [33]. Therefore, there is a possibility that LINE1 hypomethylation, which can induce its retrotranscription and transposition [34], is more strictly regulated than Alu hypomethylation.

We also showed that CT antigen genes were demethylated in a coordinated way with global hypomethylation in ESCCs and expression of these genes was consistent with methylation states of each sample by immunohistochemistry. These data suggested that CT antigen genes tended to be demethylated in ESCCs with global hypomethylation. This raises a possibility that induction of CT antigen by DNA methyltransferase inhibitors [35, 36] might lead to a more effective cancer immunotherapy targeting CT antigens.

Methylation levels of repetitive elements and CT antigen genes in ESCCs were not associated with any clinicopathological features. To exclude the possibility that a fraction of cancer cells were highly variable among the biopsy samples and made associations undetectable, we microscopically analyzed the fraction of cancer cells in biopsy samples. The fraction was 67.3 ± 6.8% (mean ± SD), and such a possibility seemed to be low. However, there still remains a possibility that use of samples with high purity, such as those prepared by laser-captured microdissection, might reveal

some weak association between hypomethylation and clinicopathological findings.

In conclusion, our study demonstrated that hypomethylation of Alu and LINE1 was present in ESCCs and that Alu hypomethylation was present even in non-cancerous background mucosae of ESCC patients. It was suggested that Alu hypomethylation represents the severity of an epigenetic field for cancerization and might become an epigenetic marker for ESCC risk estimation.

Acknowledgments This study was supported by Grants-in-Aid for the National Cancer Center Research and Development Fund, and by the Project for Development of Innovative Research on Cancer Therapeutics (P-Direct) from the Ministry of Education, Culture, Science and Sport, Japan. Y. M. and K. G. are recipients of a Research Resident Fellowship from the Foundation for Promotion of Cancer Research.

Conflict of interest The authors declare that they have no conflict of interest.

References

1. Shibata A, Matsuda T, Ajiki W, Sobue T (2008) Trend in incidence of adenocarcinoma of the esophagus in Japan, 1993–2001. Jpn J Clin Oncol 38:464–468
2. Lu CL, Lang HC, Luo JC, Liu CC, Lin HC, Chang FY, Lee SD (2009) Increasing trend of the incidence of esophageal squamous cell carcinoma, but not adenocarcinoma, in Taiwan. Cancer Causes Control 21:269–274
3. Hongo M, Nagasaki Y, Shoji T (2009) Epidemiology of esophageal cancer: orient to occident. Effects of chronology, geography and ethnicity. J Gastroenterol Hepatol 24:729–735
4. Pesko P, Rakic S, Milicevic M, Bulajic P, Gerzic Z (1994) Prevalence and clinicopathologic features of multiple squamous cell carcinoma of the esophagus. Cancer 73:2687–2690
5. Shimizu Y, Tukagoshi H, Fujita M, Hosokawa M, Kato M, Asaka M (2001) Metachronous squamous cell carcinoma of the esophagus arising after endoscopic mucosal resection. Gastrointest Endosc 54:190–194
6. Slaughter DP, Southwick HW, Smejkal W (1953) Field cancerization in oral stratified squamous epithelium; clinical implications of multicentric origin. Cancer 6:963–968
7. Ushijima T (2007) Epigenetic field for cancerization. J Biochem Mol Biol 40:142–150
8. Oka D, Yamashita S, Tomioka T, Nakanishi Y, Kato H, Kaminishi M, Ushijima T (2009) The presence of aberrant DNA methylation in noncancerous esophageal mucosae in association with smoking history: a target for risk diagnosis and prevention of esophageal cancers. Cancer 115:3412–3426
9. Lee YC, Wang HP, Wang CP, Ko JY, Lee JM, Chiu HM, Lin JT, Yamashita S, Oka D, Watanabe N et al (2011) Revisit of field cancerization in squamous cell carcinoma of upper aero digestive tract: better risk assessment with epigenetic markers. Cancer Prev Res 4:1982–1992
10. Xing EP, Nie Y, Song Y, Yang GY, Cai YC, Wang LD, Yang CS (1999) Mechanisms of inactivation of p14ARF, p15INK4b, and p16INK4a genes in human esophageal squamous cell carcinoma. Clin Cancer Res 5:2704–2713
11. Si HX, Tsao SW, Lam KY, Srivastava G, Liu Y, Wong YC, Shen ZY, Cheung AL (2001) E-cadherin expression is commonly downregulated by CpG island hypermethylation in esophageal carcinoma cells. Cancer Lett 173:71–78
12. Tanaka H, Shimada Y, Harada H, Shinoda M, Hatooka S, Imamura M, Ishizaki K (1998) Methylation of the 5′ CpG island of the FHIT gene is closely associated with transcriptional inactivation in esophageal squamous cell carcinomas. Cancer Res 58:3429–3434
13. Wong ML, Tao Q, Fu L, Wong KY, Qiu GH, Law FB, Tin PC, Cheung WL, Lee PY, Tang JC et al (2006) Aberrant promoter hypermethylation and silencing of the critical 3p21 tumour suppressor gene, RASSF1A, in Chinese oesophageal squamous cell carcinoma. Int J Oncol 28:767–773
14. Feinberg AP, Vogelstein B (1983) Hypomethylation distinguishes genes of some human cancers from their normal counterparts. Nature 301:89–92
15. Jones PA, Baylin SB (2007) The epigenomics of cancer. Cell 128:683–692
16. Ehrlich M (2002) DNA methylation in cancer: too much, but also too little. Oncogene 21:5400–5413
17. De Smet C, De Backer O, Faraoni I, Lurquin C, Brasseur F, Boon T (1996) The activation of human gene MAGE-1 in tumor cells is correlated with genome-wide demethylation. Proc Natl Acad Sci USA 93:7149–7153
18. Kaneda A, Tsukamoto T, Takamura-Enya T, Watanabe N, Kaminishi M, Sugimura T, Tatematsu M, Ushijima T (2004) Frequent hypomethylation in multiple promoter CpG islands is associated with global hypomethylation, but not with frequent promoter hypermethylation. Cancer Sci 95:58–64
19. Yang AS, Estecio MR, Doshi K, Kondo Y, Tajara EH, Issa JP (2004) A simple method for estimating global DNA methylation using bisulfite PCR of repetitive DNA elements. Nucleic Acids Res 32:e38
20. Weisenberger DJ, Campan M, Long TI, Kim M, Woods C, Fiala E, Ehrlich M, Laird PW (2005) Analysis of repetitive element DNA methylation by MethyLight. Nucleic Acids Res 33:6823–6836
21. Caballero OL, Chen YT (2009) Cancer/testis (CT) antigens: potential targets for immunotherapy. Cancer Sci 100:2014–2021
22. Gnjatic S, Nishikawa H, Jungbluth AA, Gure AO, Ritter G, Jager E, Knuth A, Chen YT, Old LJ (2006) NY-ESO-1: review of an immunogenic tumor antigen. Adv Cancer Res 95:1–30
23. Nuber N, Curioni-Fontecedro A, Matter C, Soldini D, Tiercy JM, von Boehmer L, Moch H, Dummer R, Knuth A, van den Broek M (2010) Fine analysis of spontaneous MAGE-C1/CT7-specific immunity in melanoma patients. Proc Natl Acad Sci USA 107:15187–15192
24. Chen RZ, Pettersson U, Beard C, Jackson-Grusby L, Jaenisch R (1998) DNA hypomethylation leads to elevated mutation rates. Nature 395:89–93
25. Eden A, Gaudet F, Waghmare A, Jaenisch R (2003) Chromosomal instability and tumors promoted by DNA hypomethylation. Science 300:455
26. Gaudet F, Hodgson JG, Eden A, Jackson-Grusby L, Dausman J, Gray JW, Leonhardt H, Jaenisch R (2003) Induction of tumors in mice by genomic hypomethylation. Science 300:489–492
27. Kaneda A, Kaminishi M, Sugimura T, Ushijima T (2004) Decreased expression of the seven ARP2/3 complex genes in human gastric cancers. Cancer Lett 212:203–210
28. Yoshida T, Yamashita S, Takamura-Enya T, Niwa T, Ando T, Enomoto S, Maekita T, Nakazawa K, Tatematsu M, Ichinose M et al (2011) Alu and Satalpha hypomethylation in Helicobacter pylori-infected gastric mucosae. Int J Cancer 128:33–39
29. Wilson AS, Power BE, Molloy PL (2007) DNA hypomethylation and human diseases. Biochim Biophys Acta 1775:138–162

30. Kim BH, Cho NY, Shin SH, Kwon HJ, Jang JJ, Kang GH (2009) CpG island hypermethylation and repetitive DNA hypomethylation in premalignant lesion of extrahepatic cholangiocarcinoma. Virchows Arch 455:343–351
31. Ogino S, Nosho K, Kirkner GJ, Kawasaki T, Chan AT, Schernhammer ES, Giovannucci EL, Fuchs CS (2008) A cohort study of tumoral LINE-1 hypomethylation and prognosis in colon cancer. J Natl Cancer Inst 100:1734–1738
32. Dewannieux M, Esnault C, Heidmann T (2003) LINE-mediated retrotransposition of marked Alu sequences. Nat Genet 35:41–48
33. Belancio VP, Hedges DJ, Deininger P (2008) Mammalian non-LTR retrotransposons: for better or worse, in sickness and in health. Genome Res 18:343–358
34. Bourc'his D, Bestor TH (2004) Meiotic catastrophe and retrotransposon reactivation in male germ cells lacking Dnmt3L. Nature 431:96–99
35. Guo ZS, Hong JA, Irvine KR, Chen GA, Spiess PJ, Liu Y, Zeng G, Wunderlich JR, Nguyen DM, Restifo NP et al (2006) De novo induction of a cancer/testis antigen by 5-aza-2′-deoxycytidine augments adoptive immunotherapy in a murine tumor model. Cancer Res 66:1105–1113
36. Oi S, Natsume A, Ito M, Kondo Y, Shimato S, Maeda Y, Saito K, Wakabayashi T (2009) Synergistic induction of NY-ESO-1 antigen expression by a novel histone deacetylase inhibitor, valproic acid, with 5-aza-2′-deoxycytidine in glioma cells. J Neurooncol 92:15–22

IJC
International Journal of Cancer

The tumor suppressor *microRNA-29c* is downregulated and restored by celecoxib in human gastric cancer cells

Yoshimasa Saito[1,2], Hidekazu Suzuki[1], Hiroyuki Imaeda[1], Juntaro Matsuzaki[1], Kenro Hirata[1], Hitoshi Tsugawa[1], Sana Hibino[2], Yae Kanai[3], Hidetsugu Saito[1,2] and Toshifumi Hibi[1]

[1] Division of Gastroenterology and Hepatology, Department of Internal Medicine, Keio University School of Medicine, Shinjuku-ku, Tokyo, Japan
[2] Division of Pharmacotherapeutics, Keio University Faculty of Pharmacy, Minato-ku, Tokyo, Japan
[3] Pathology Division, National Cancer Center Research Institute, Chuo-ku, Tokyo, Japan

MicroRNAs (miRNAs) are small noncoding RNAs that function as endogenous silencers of target genes and play critical roles during carcinogenesis. The selective cyclooxygenase-2 (COX-2) inhibitor celecoxib has been highlighted as a potential drug for treatment of gastrointestinal tumors. The aim of this study was to investigate the role of miRNAs in gastric carcinogenesis and the feasibility of a new therapeutic approach for gastric cancer. miRNA expression profiles were examined in 53 gastric tumors including gastric adenomas (atypical epithelia), early gastric cancers and advanced gastric cancers and in gastric cancer cells treated with celecoxib. miRNA microarray analysis revealed that *miR-29c* was significantly downregulated in gastric cancer tissues relative to nontumor gastric mucosae. *miR-29c* was significantly activated by celecoxib in gastric cancer cells. Downregulation of *miR-29c* was associated with progression of gastric cancer and was more prominent in advanced gastric cancers than in gastric adenomas and early gastric cancer. In addition, expression of the oncogene *Mcl-1*, a target of *miR-29c*, was significantly increased in gastric cancer tissues relative to nontumor gastric mucosae. Activation of *miR-29c* by celecoxib induced suppression of Mcl-1 and apoptosis in gastric cancer cells. These results suggest that downregulation of the tumor suppressor *miR-29c* plays critical roles in the progression of gastric cancer. Selective COX-2 inhibitors may have clinical promise for the treatment of gastric cancer via restoration of *miR-29c*.

MicroRNAs (miRNAs) are small noncoding RNAs that function as endogenous silencers of various target genes. Hundreds of human miRNAs have been identified in the human genome, being expressed in a tissue-specific manner and playing important roles in cell proliferation, apoptosis and differentiation during mammalian development.[1] Links between miRNAs and the development and progression of human malignancies are becoming increasingly apparent, especially with regard to aberrant expression of miRNAs.[2,3] We have recently reported that some miRNAs are regulated by epigenetic alterations such as DNA methylation and histone modification at their CpG island promoters and that epigenetic activation of tumor suppressor miRNAs may be a novel therapeutic approach for human cancers.[4–7] We have also reported that miRNAs may play important roles in the pathogenesis of not only malignancies but also functional gastrointestinal disorders such as functional dyspepsia.[8]

Gastric cancer is the second most common cause of cancer-related death worldwide.[9,10] Advanced gastric cancer is defined as adenocarcinoma with invasion to the muscularis propria or deeper gastric wall. Although patients who are diagnosed as having gastric cancer at an advanced stage undergo surgical resection and systemic chemotherapy, their prognosis is generally poor. However, early gastric cancer is defined as adenocarcinoma confined to the mucosa or submucosa of the stomach and can be treated using endoscopic submucosal dissection (ESD), which is an advanced therapeutic technique that can offer extremely promising outcomes.[11,12] Examination of miRNA expression profiles has revealed that specific miRNAs are aberrantly expressed in various human cancers.[2,13,14]

Cyclooxygenase (COX) is a critical enzyme involved in prostaglandin production and has two isoforms: COX-2,

Key words: microRNA, *miR-29c*, gastric cancer, *Mcl-1*, celecoxib
Abbreviations: ChIP: chromatin immunoprecipitation; COX: cyclooxygenase; ESD: endoscopic submucosal dissection; *H. pylori*: *Helicobacter pylori*; HE: hematoxylin-eosin; ISH: *in situ* hybridization; miRNA: microRNA
Additional Supporting Information may be found in the online version of this article.
Conflict of interest: All the authors have declared no conflict of interest.
Grant sponsor: Japan Society for Promotion of Science (JSPS), Grant-in-Aid for Young Scientists A; Grant number: 23680090; Grant sponsor: JSPS, Grant-in-Aid for Scientific Research B; Grant number: 22300169; Grant sponsors: Takeda Science Foundation, Sagawa Foundation for Promotion of Cancer Research, Smoking Research Foundation, Keio Gijuku Academic Development Funds
DOI: 10.1002/ijc.27862
History: Received 23 May 2012; Accepted 10 Sep 2012; Online 24 Sep 2012
Correspondence to: Hidekazu Suzuki, Division of Gastroenterology and Hepatology, Department of Internal Medicine, Keio University School of Medicine, 35 Shinanomachi, Shinjuku-ku, Tokyo 160-8582, Japan, Tel.: +813-5363-3914, Fax: +813-5363-3967, E-mail: hsuzuki@a6.keio.jp

What's new?

MicroRNAs (miRNAs) play critical roles in carcinogenesis and may be valuable therapeutic targets for malignant disease. Here, the miRNA tumor suppressor miR-29c was found to be significantly downregulated in gastric cancer cells and to be reactivated by the selective cyclooxygenase-2 (COX-2) inhibitor celecoxib. Reactivation led to miR-29c-induced suppression of the anti-apoptotic protein Mcl-1. The data reveal that selective COX-2 inhibitors may have clinical promise for the treatment of gastric cancer via restoration of miR-29c.

which is commonly overexpressed in solid tumors including gastric cancer, and COX-1, which is expressed constitutively in normal tissues, suggesting that inhibition of COX-2 may reduce the risk of cancer development. Clinical trials have revealed that the selective COX-2 inhibitor celecoxib is effective for prevention of colorectal adenomas.[15,16] Recent studies have also shown that celecoxib has a preventive effect against *Helicobacter pylori*-associated gastric cancer.[17,18] Therefore, celecoxib has been suggested to have promise for the treatment of gastrointestinal tumors. However, the molecular mechanisms underlying the chemopreventive effects of selective COX-2 inhibitors are not fully understood.

To identify miRNAs that play critical roles in the development and progression of gastric cancer, we examined the miRNA expression profiles of gastric tumors including gastric adenomas and both early and advanced gastric cancers. We also investigated miRNAs that are targeted by celecoxib. Our findings revealed that *miR-29c* was downregulated in gastric cancers and activated by celecoxib. Recent studies have shown that *miR-29c* is downregulated in various human malignancies including gastric cancer and acts as a tumor suppressor.[19–25] Herein, we show that the putative tumor suppressor *miR-29c* is an important miRNA in gastric carcinogenesis and is a potential therapeutic target for gastric cancer.

Material and Methods

Patients and tissue specimens

A total of 53 clinical samples of gastric tumors were examined. The clinicopathological features of the patients are shown in Supporting Information Table 1. The average age of the patients was 67.7 years (male/female, 39/14). Thirty patients with gastric adenomas (atypical epithelium) or early gastric cancers underwent ESD at Keio University Hospital (Tokyo, Japan). This study was approved by the research ethics committee of Keio University School of Medicine (#19-68-5) and registered with the UMIN Clinical Trials Registry (UMIN 000001057). Informed consent was obtained from all patients before the examinations. Tissue specimens from gastric adenomas and early gastric cancers and the surrounding nontumor gastric mucosae were obtained by endoscopic biopsy and kept in RNAlater (Ambion, Austin, TX) at −80°C until RNA extraction. Tissue specimens from advanced gastric cancers and the surrounding nontumor gastric mucosae were obtained from materials surgically resected from 23 patients at the National Cancer Center Hospital (Tokyo, Japan). This study was approved by the Ethics Committee of the National Cancer Center and performed in accordance with the 1964 Declaration of Helsinki. All patients gave their informed consent for inclusion in this study.

Cell lines and treatment with celecoxib

The human gastric cancer cell lines AGS and MKN45 were used in this study. AGS was obtained from the American Type Culture Collection (Rockville, MD), and MNK45 was obtained from the Japan Health Science Foundation (Osaka, Japan). Cells were cultured in RPMI1640 medium supplemented with 10% fetal bovine serum and seeded at 1×10^5 cells per 100-mm dish 24 hr prior to treatment. Cells were treated with celecoxib (Pfizer, New York, NY) at 30 μM for 48 hr.

RNA extraction and microarray analysis

Total RNAs were extracted from both tissue specimens of gastric tumors resected by ESD and gastric cancer cell lines using the mirVana miRNA isolation kit (Ambion). Total RNA of tissue specimens from advanced gastric cancers and matched nontumor gastric mucosae was extracted using TRIzol reagent (Invitrogen, Carlsbad, CA).

Five hundred nanograms of total RNA from each of ten advanced gastric cancers were pooled, and the same was done with 10 matched nontumor gastric mucosae. miRNA microarray analysis of samples of advanced gastric cancer was conducted by Toray Industries (www.toray.com: Tokyo, Japan). miRNA microarray analysis of AGS cells treated with celecoxib was conducted by LC Sciences (www.lcsciences.com: Houston, TX). All data were submitted to the ArrayExpress database, under the accession numbers E-MEXP-2230 (gastric cancer) and E-MEXP-2231 (celecoxib). These microarray chips contain probe regions that detect 724 (Toray Industries) and 711 (LC Sciences) miRNA transcripts listed in Sanger miRBase Release 10.0 (http://www.sanger.ac.uk). These chips contain multiple probes for each miRNA (2 probes in the Toray Industries chip, 5 probes in the LC Sciences chip), and the average values of their signal intensities are shown in Tables 1 and 3.

Quantitative RT-PCR of miR-29c

Levels of miRNA expression were analyzed by quantitative RT-PCR using the TaqMan microRNA assay for *miR-29c* (Applied Biosystems, Foster City, CA) in accordance with the manufacturer's instructions. Expression levels were normalized to that of U6 RNA.

Table 1. Summary of the most downregulated miRNAs in advanced gastric cancers relative to non-tumorous gastric mucosae

No.	miRNAs	Non-tumor	Tumor	Fold change
1	*miR-193b*	1133.8	563.0	0.5
2	*miR-768–3p*	756.8	372.1	0.5
3	*miR-140–3p*	1438.6	690.7	0.5
4	*miR-923*	43834.8	20277.2	0.5
5	*miR-939*	3780.0	1655.2	0.4
6	*miR-487b*	173.0	72.2	0.4
7	*miR-378**	95.3	39.6	0.4
8	*miR-29c*	1733.9	641.1	0.4
9	*miR-133b*	424.6	155.0	0.4
10	*miR-768–5p*	1499.5	518.1	0.3

Note: Data for Non-tumor and Tumor are average values of the signal intensities in microarray analysis. Fold change represents the ratio of the signal intensities for Tumor/Non-tumor.

In situ hybridization (ISH) of miR-29c

Locked nucleic acid (LNA)-modified probes for *miR-29c* were used (miRCURY-LNA detection probe, Exiqon, Vedbaek, Denmark). *In situ* hybridization was performed using the RiboMap *in situ* hybridization kit (Ventana Medical Systems, Tucson, AZ) on the Ventana Discovery automated *in situ* hybridization instrument (Ventana Medical Systems). *In situ* hybridization steps after deparaffinization were performed based on the standard protocol provided in the manufacturer's RiboMap application note (http://www.ventanamed.com). Hematoxylin-eosin (HE) was used for counterstaining.

Immunohistochemical examination of Mcl-1

Formalin-fixed and paraffin-embedded tissues were deparaffinized and rehydrated. For antigen retrieval, the sections were treated for 10 min at 105°C in an autoclave, and nonspecific reactions were blocked with a blocking reagent (Protein Block Serum-Free, Dako Cytomation, Glostrup, Denmark). The sections were incubated with the rabbit anti-human Mcl-1 polyclonal antibody (S-19, Santa Cruz Biotechnology, Santa Cruz, CA) overnight at 4°C followed by horseradish peroxidase labeled anti-rabbit IgG (Histofine, Simple stain MAX-PO, Nichirei, Tokyo, Japan) for 30 min at room temperature. Then, the sections were treated with 3.3′-diaminobenzidine tetrahydrochloride solution. All sections were counterstained with hematoxylin.

Immunoreactivity of Mcl-1 was confirmed in the germinal centers as described previously,[26] and this was defined as the internal positive control. The intensity of Mcl-1 immunoreactivity in each sample was graded as 0 (less than the internal positive control), 1 (equal to the internal positive control) and 2 (more than the internal positive control). Mcl-1 expression in randomly selected fields, two in gastric cancer tissues and two in nontumor gastric mucosal tissues, was examined in gastric adenomas and early ($n = 30$) and advanced ($n = 21$) gastric cancers at high magnification (×400). The Mcl-1 expression score was determined as the product of the Mcl-1 immunoreactivity grade and the percentage of Mcl-1-positive cells.

Chromatin immunoprecipitation (ChIP) assay

The ChIP assay was performed as described previously.[4] An antibody against C/EBPα (sc-61, Santa Cruz Biotechnology) was used. Quantitative analysis was performed by real-time PCR with the CYBR Premix Ex Taq (Takara Bio, Ohtsu, Japan) using the Thermal Cycler Dice Real-Time System (Takara Bio). The sequences of the primers used were as follows; Forward: 5′-CTAAGAGCAGACTGATGGTGTC-3′, Reverse: 5′-CTATTTCTGTTGACTCCTAGCAGC-3′.

The fraction of immunoprecipitated DNA was calculated as follows: [immunoprecipitated DNA with C/EBPα antibody–nonspecific antibody control (NAC)]/(input DNA – NAC).

Western blotting

Protein extracts were separated by SDS/polyacrylamide gel electrophoresis and transferred onto nitrocellulose membranes. The membranes were hybridized with a rabbit anti-human Mcl-1 polyclonal antibody (S-19, Santa Cruz Biotechnology), and β-actin was used as the internal control.

Transfection of miR-29c precursor molecules and the specific miR-29c inhibitor

The *miR-29c* precursor molecules, the specific *miR-29c* inhibitor and negative control precursor miRNAs were purchased from Ambion. They were transfected into AGS and MKN45 cells at a final concentration of 100 nM each using oligofectamine (Invitrogen) in accordance with the manufacturer's instructions. Forty-eight hours after transfection, the cells were collected and their expression of Mcl-1 was analyzed by Western blotting as described above.

Apoptosis assay

The levels of apoptosis in AGS and MKN45 cells transfected with *miR-29c* and treated with celecoxib were evaluated using Annexin V kit (Beckman Coulter, Brea CA) in accordance with the manufacturer's instructions.

Statistics

Data were analyzed using the SPSS statistics 17.0 software package. Differences in miRNA expression levels and apoptosis levels between groups were analyzed using unpaired t test. Differences at $p < 0.05$ were considered significant.

Results

Downregulation of miR-29c is associated with progression of gastric cancer

To investigate the miRNA expression profile in gastric cancer, we compared the miRNA expression of gastric cancer tissues with that of the corresponding nontumorous gastric mucosae. The microarray data shown in Table 1 revealed that the putative tumor suppressor *miR-29c* was significantly

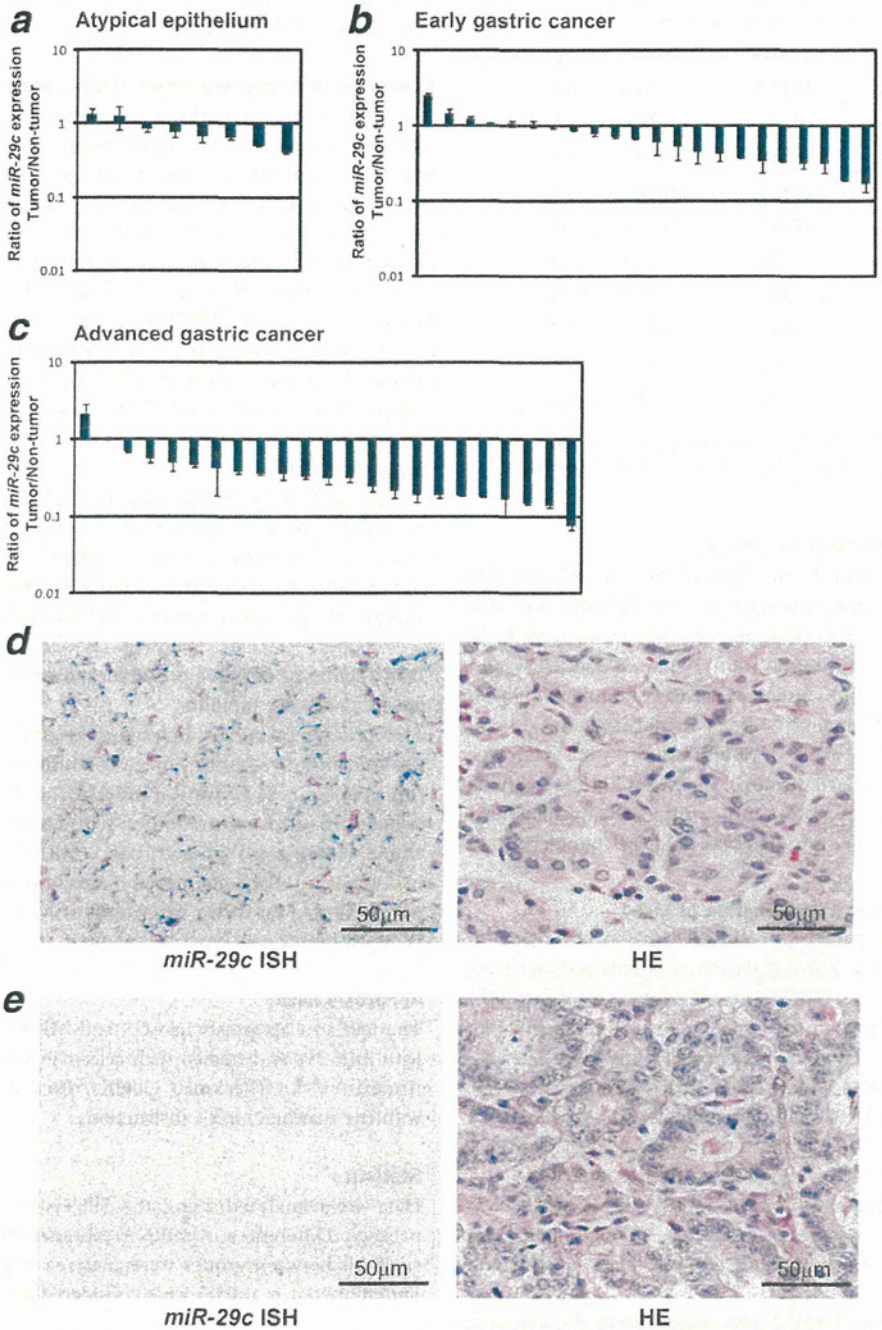

Figure 1. The expression levels of *miR-29c* in the 53 clinical gastric tumor samples and matched nontumorous gastric mucosae. All reactions were performed in duplicate with U6 as the internal control. The graph shows the ratio of *miR-29c* expression of tumor/nontumor on a logarithmic scale (mean ± SD). (*a*) Gastric adenomas (atypical epithelium, $n = 8$). There was no significant association of *miR-29c* expression between tumor and nontumor. (*b*) Early gastric cancers ($n = 22$). The expression levels of *miR-29c* in early gastric cancers were significantly lower than those in the corresponding nontumorous gastric mucosae ($p < 0.005$). (*c*) Advanced gastric cancers ($n = 23$). The expression levels of *miR-29c* in advanced gastric cancers were significantly lower than those in the corresponding nontumorous gastric mucosae ($p < 0.0005$). (*d*) A representative example of ISH for *miR-29c* in normal gastric tissue. *miR-29c* is expressed in the cytoplasm of normal gastric epithelial cells (blue staining) but not detected in other cells such as fibroblasts and muscle cells. HE was used for counterstaining. (*e*) A representative example of ISH for *miR-29c* in gastric cancer tissue. *miR-29c* expression was not detected in gastric cancer cells. HE was used for counterstaining.

downregulated in gastric cancer tissues relative to nontumorous gastric mucosae. To confirm the microarray data, we examined the levels of *miR-29c* expression in tissue specimens of gastric adenomas (atypical epithelium), early gastric cancers and advanced gastric cancers by quantitative RT-PCR. As shown in Figure 1*a*, the expression level of *miR-29c* was reduced in 75% (6 of 8) of gastric adenomas compared with the corresponding nontumor gastric mucosae. There was no significant difference in the average level of *miR-29c* expression between gastric adenomas and the corresponding nontumor gastric mucosae. The expression level of *miR-29c* was reduced in 73% (16 of 22) of early gastric cancers compared with the corresponding nontumor gastric mucosae (Fig. 1*b*), and the expression levels of *miR-29c* in early gastric cancers were significantly lower than those in the corresponding nontumorous gastric mucosae ($p < 0.005$). Furthermore, the expression level of *miR-29c* was reduced in 91% (21 of 23) of advanced gastric cancers relative to the corresponding nontumorous gastric tissues (Fig. 1*c*), and this reduction was shown to be significant ($p < 0.0005$). The relative expression levels of *miR-29c* in nontumorous gastric mucosa and gastric tumors and the ratio of *miR-29c* expression on a linear scale are shown in Supporting Information Figure 1.

To confirm the localization of *miR-29c* in gastric cancer tissues, ISH for *miR-29c* was performed. Figures 1*d* and 1*e* show representative examples of ISH for *miR-29c*. *miR-29c* is expressed in the cytoplasm of normal gastric epithelial cells (blue staining) but not detected in other cells such as fibroblasts and muscle cells. *miR-29c* expression was not detected in gastric cancer cells. These results are consistent with the data for quantitative RT-PCR of *miR-29c*.

We also examined the association between the ratio of *miR-29c* expression and clinicopathological features such as tumor differentiation, tumor location, *H. pylori* infection and clinical stage. We found that downregulation of *miR-29c* was more prominent in undifferentiated than in differentiated advanced gastric cancers (Table 2, Supporting Information Fig. 1). There was no significant association between the ratio of *miR-29c* expression and other clinicopathological features such as tumor location, *H. pylori* infection and clinical stage (Table 2).

Table 2. Association between the ratio of *miR-29c* expression and clinicopathological features of patients with gastric cancer

	N	Ratio of *miR-29c* expression (T/N)	*p*-value
a) Early gastric cancer			
Tumor differentiation			
Differentiated	19	0.75 ± 0.13	$p = 0.98$
Undifferentiated	3	0.76 ± 0.27	
Tumor location			
Upper and Middle portion	3	0.98 ± 0.14	$p = 0.23$
Lower portion	19	0.72 ± 0.13	
H.pylori infection			
Positive	10	0.88 ± 0.23	$p = 0.51$
Negative	10	0.71 ± 0.11	
b) Advanced gastric cancer			
Tumor differentiation			
Differentiated	14	0.54 ± 0.14	$p = 0.04$[1]
Undifferentiated	9	0.22 ± 0.04	
Tumor location			
Upper and Middle portion	13	0.45 ± 0.15	$p = 0.65$
Lower portion	10	0.37 ± 0.08	
T stage			
T1, T2	9	0.58 ± 0.21	$p = 0.25$
T3, T4	14	0.31 ± 0.05	
Clinical stage			
I, II, III	13	0.30 ± 0.05	$p = 0.22$
IV	10	0.56 ± 0.19	

Note: The ratios of *miR-29c* expression (Tumor/Non-tumor) are expressed as mean ± SE. Differences between groups were analyzed by unpaired t test.
[1]There was a significant correlation between the ratio of *miR-29c* expression and tumor differentiation.

Increased expression of Mcl-1, a target gene of miR-29c, in gastric cancer tissues

We next investigated the target genes of *miR-29c*. Mott *et al.*[19] have demonstrated that Mcl-1, encoding an antiapoptotic Bcl2 family protein, is one of the targets of *miR-29* miRNAs, and that *miR-29* miRNAs regulate apoptosis by targeting Mcl-1. The levels of Mcl-1expression in gastric cancer tissues were examined by immunohistochemistry. Immunoreactivity of the Mcl-1 antibody was confirmed by staining of the germinal centers, as described previously (Fig. 2*a*).[26] Prominent staining of Mcl-1 was observed in the cytoplasm of gastric cancer cells. Expression of Mcl-1 was markedly increased in advanced gastric cancer (Figs. 2*c* and 2*d*), whereas in nontumorous gastric tissues only faint staining was evident (Fig. 2*b*). Mcl-1 expression was also increased in early gastric cancer (Fig. 2*e*).

The degree of Mcl-1 overexpression was represented as the ratio of the Mcl-1 expression score between the tumor and nontumorous mucosa (*T/N*). The average value of the ratio of Mcl-1 expression (*T/N*) in advanced gastric cancers was significantly higher than that in gastric adenomas and early gastric cancers (Fig. 2*f*).

miR-29c is activated by the selective COX-2 inhibitor celecoxib and suppresses Mcl-1

To identify miRNAs that are differentially expressed upon treatment of AGS gastric cancer cells with the selective COX-2 inhibitor celecoxib, we performed miRNA microarray

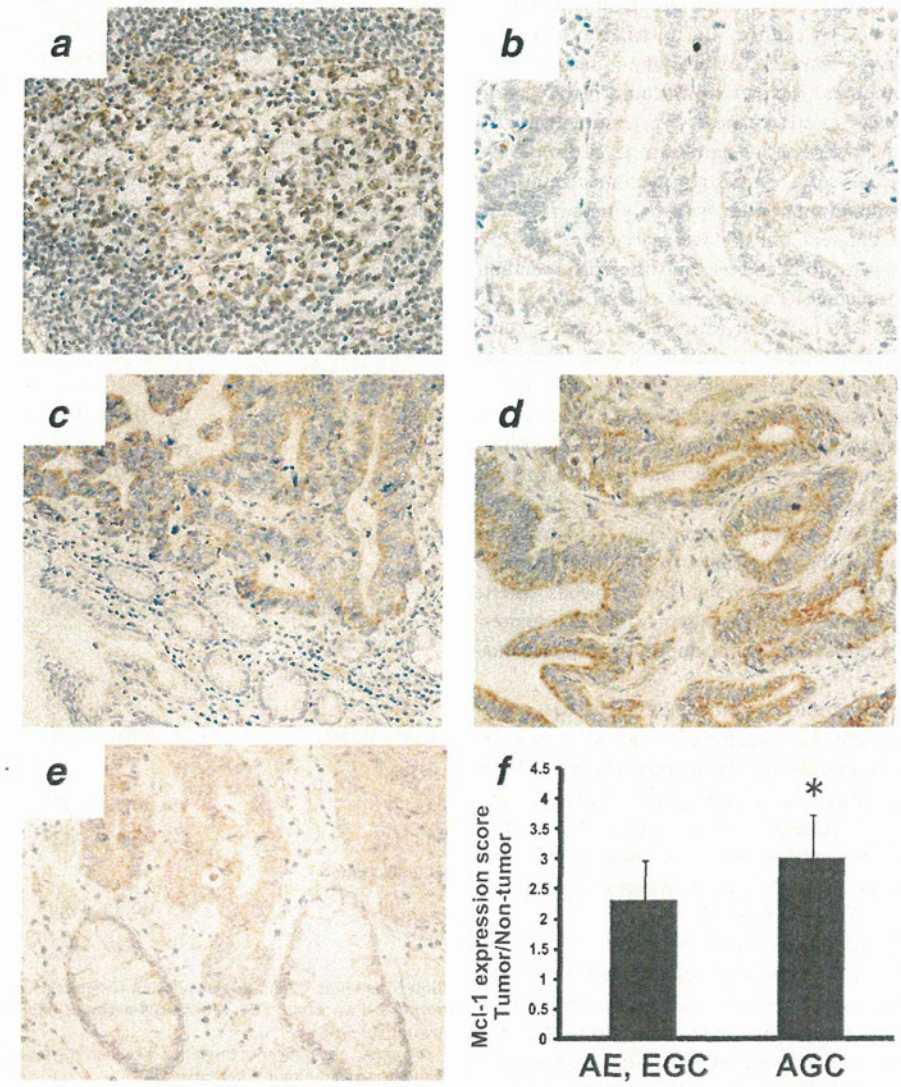

Figure 2. Expression levels of Mcl-1 in gastric cancer tissues examined by immunohistochemistry. (*a*) Immunoreactivity of the Mcl-1 antibody was confirmed by staining of the germinal centers as described previously.[26] Immunohistochemical examinations of Mcl-1 in nontumorous gastric tissues (*b*), advanced gastric cancer (*c*, *d*) and early gastric cancer (*e*) are shown. (*f*) The average levels of the ratio of the Mcl-1 expression score (*T*/*N*) in gastric cancer. AE: atypical epithelium; AGC: advanced gastric cancer; ECG: early gastric cancer. $*p < 0.05$.

analysis. As shown in Table 3, *miR-29c*, which is downregulated in gastric cancer tissues, was significantly activated after treatment with celecoxib.

Figure 3*a* shows the expression levels of *miR-29c* in AGS and MKN45 gastric cancer cells treated with celecoxib. The expression levels of *miR-29c* in AGS and MKN45 cells treated with celecoxib were significantly higher than those in untreated cells ($p < 0.05$), being consistent with the microarray data. We also examined the expression levels of *miR-29c* in AGS and MKN45 cells after treatment with celecoxib in the presence of the specific *miR-29c* inhibitor. We confirmed that increased expression of *miR-29c* by celecoxib was cancelled after transfection with the specific *miR-29c* inhibitor.

We next examined the expression levels of Mcl-1, a target of *miR-29c*, by Western blotting in AGS and MKN45 cells after transfection with the *miR-29c* precursor molecules and treatment with celecoxib with or without the specific *miR-29c* inhibitor. We measured the expression levels of *miR-29c* after its transfection and confirmed that *miR-29c* expression was markedly increased (over 100-fold) after transfection. The results of Western blotting showed that the expression levels of Mcl-1 in AGS and MKN45 cells treated with celecoxib and transfected with the *miR-29c* precursor molecules were

Table 3. Summary of the most upregulated miRNAs in AGS cells treated with celecoxib

No.	miRNAs	Control	Celecoxib	Fold change
1	*miR-663*	206.8	935.1	4.5
2	*miR-181b*	90.4	395.9	4.4
3	*miR-29c*	497.0	1972.0	4.0
4	*miR-141*	122.5	410.3	3.3
5	*miR-149**	285.8	894.4	3.1
6	*miR-98*	392.9	1113.9	2.8
7	*miR-26b*	593.4	1340.3	2.3
8	*miR-195*	279.4	626.5	2.2
9	*miR-148a*	333.1	707.6	2.1
10	*miR-638*	3682.7	7073.3	1.9

Note: Data for Control and Celecoxib are average values of the signal intensities in microarray analysis. Fold change represents the ratio of the signal intensities for Celecoxib/Control.

lower than in the control. We confirmed that suppression of Mcl-1 by celecoxib was cancelled after transfection with the specific *miR-29c* inhibitor, suggesting that celecoxib-induced suppression of Mcl-1 is mediated by *miR-29c* (Fig. 3*b*)

Celecoxib activates miR-29c expression by enhancing the DNA binding of C/EBPα to the promoter

The results of microarray analysis revealed that celecoxib activates the expression of *miR-29c*, but not that of *miR-29b*, suggesting that celecoxib may modulate the binding of transcriptional factors between *miR-29b* and *miR-29c* (Fig. 3*c*). Using the database (www.gene-regulation.com/pub/programs.html), we found that there are C/EBPα binding sites in the promoter region of *miR-29c*. Moreover, Wu *et al.* have reported that celecoxib induces the expression of the invasion-suppressor CRMP-1 by enhancing the binding of C/EBPα DNA to the promoter.[27] These findings prompted us to perform a ChIP assay with the C/EBPα antibody in AGS and MKN45 cells treated with celecoxib. As shown in Figure 3*c*, the results of the ChIP assay showed that immunoprecipitation with the C/EBPα antibody was significantly increased in AGS and MKN45 cells treated with celecoxib, indicating that celecoxib activates the expression of *miR-29c* by enhancing the binding of C/EBPα DNA to the promoter.

Celecoxib and miR-29c induce apoptosis in gastric cancer cells

Since Mcl-1 is an antiapoptotic factor and suppressed by *miR-29c* in gastric cancer cells, we performed annexin V-FITC apoptosis assay in AGS and MKN45 cells. Fluorescence microscopy and flow cytometry analyses demonstrated that annexin V staining (green staining on the cell surface membrane) was markedly increased in AGS and MKN45 cells 48 hr after *miR-29c* transfection and celecoxib treatment, indicating that *miR-29c* and celecoxib induce apoptosis in gastric cancer cells (Fig. 4).

Discussion

We focused our study on *miR-29c*, because it was the only miRNA that was highlighted by the results of the two microarray analyses. Although the extent of these analyses was intrinsically limited, the results suggested that *miR-29c* is downregulated in gastric cancer and reactivated by celecoxib.

Gastric adenomas and early gastric cancers are clinically similar gastric neoplasms, and sometimes they are difficult to diagnose only by endoscopic findings even with biopsied pathological examination. Therefore, the significant reduction of *miR-29c* expression in early gastric cancers, but not in gastric adenomas, suggests that *miR-29c* could be a novel molecular marker of early gastric cancer. Moreover, reduction of *miR-29c* expression is more prominent in advanced gastric cancers than in gastric adenomas and early gastric cancers. These findings suggest that reduction of *miR-29c* expression is critical for the progression of gastric cancer.

Downregulation of *miR-29c* has been reported in various human malignancies including nasopharyngeal carcinoma,[20] bladder transitional cell carcinoma,[21] esophageal cancer,[22] chronic lymphocytic leukemia[23,24] and gastric cancer.[25] Mott *et al.*[19] have demonstrated that Mcl-1, encoding an antiapoptotic Bcl2 family protein, is one of the targets of *miR-29* miRNAs, and that *miR-29* miRNAs regulate apoptosis by targeting Mcl-1. Mcl-1 is an antiapoptotic protein originally isolated from the ML-1 human myeloid leukemia cell line during cell differentiation.[28] The biological relevance of Mcl-1 as an antiapoptotic protein promoting cell survival has been reported in various human malignancies.[29–31] Elevated expression of Mcl-1 and its association with poor prognosis have been reported in gastric cancer.[32,33] In accordance with these reports, our results demonstrate that *miR-29c* is downregulated in gastric cancers and suppresses its target oncogene, *Mcl-1*. In addition, downregulation of *miR-29c* and overexpression of Mcl-1 are associated with the progression of gastric cancer. These findings suggest that *miR-29c* functions as a tumor suppressor by suppressing Mcl-1 in gastric epithelial cells. We and other groups have previously shown that other miRNAs such as *miR-512-5p* and transcription factors also regulate *Mcl-1* expression.[7] Further studies are necessary to examine other miRNAs and/or transcription factors that regulate Mcl-1 expression in gastric epithelial cells.

Our data from this study showed that the selective COX-2 inhibitor celecoxib activated the expression of *miR-29c* and suppressed its target oncogene *Mcl-1*, resulting in induction of apoptosis in gastric cancer cells. We confirmed that suppression of Mcl-1 by celecoxib was cancelled after transfection with the specific *miR-29c* inhibitor. These results suggest that suppression of Mcl-1 and induction of apoptosis in gastric cancer cells by celecoxib are mediated by *miR-29c*. Since celecoxib is a selective COX-2 inhibitor frequently used for treatment of pain, fever and inflammation, it can prevent side effects of other anticancer drugs. Combination treatment with celecoxib and other anticancer drugs may be beneficial for reducing side effects and achieving more potent activity against gastric cancer.

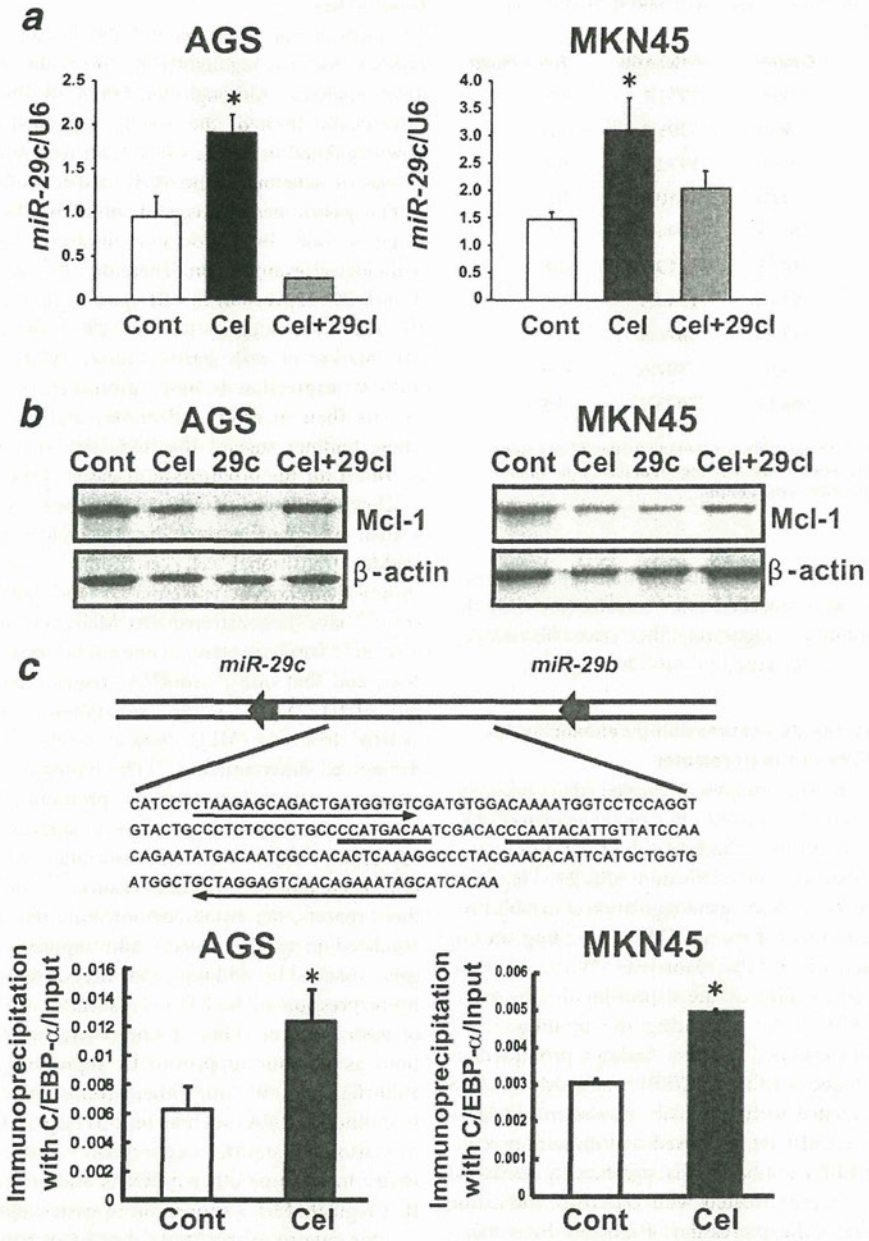

Figure 3. *miR-29c* is activated by celecoxib and suppresses Mcl-1. (*a*) The expression levels of *miR-29c* in AGS and MKN45 cells treated with celecoxib with or without the specific *miR-29c* inhibitor. Cont: control; Cel: celecoxib; Cel+29cI: celecoxib with *miR-29c* inhibitor. *$p < 0.05$ compared with control. (*b*) Western blotting for expression levels of Mcl-1 in AGS and MKN45 cells after transfection with the *miR-29c* precursor molecules and treatment with celecoxib with or without the specific *miR-29c* inhibitor. 29c: miR-29c; Cel+29cI: celecoxib with miR-29c inhibitor; Cel: celecoxib; Cont: control. β-actin was used as the internal control. (*c*) ChIP assay with the C/EBPα antibody in AGS and MKN45 cells treated with celecoxib. The database shows that there are C/EBPα binding sites in the promoter region of *miR-29c* (www.gene-regulation.com/pub/programs.html). Arrows show the primers used for the ChIP assay. Underlining shows the C/EBPα binding sites. Immunoprecipitation with the C/EBPα antibody was significantly increased in AGS and MKN45 cells treated with celecoxib (*$p < 0.05$).

The miRNA expression profiles shown in this study, and in other reports, have demonstrated that *miR-29b* and *miR-29c* have different expression patterns, suggesting that *miR-29c* has a unique promoter in gastric cancer cells. The results of ChIP assay indicated that celecoxib activates *miR-29c* expression by enhancing the binding of C/EBPα DNA at the promoter. Selective COX-2 inhibitors may activate the tumor suppressor *miR-29c* via C/EBPα and induce apoptosis of gastric cancer cells.

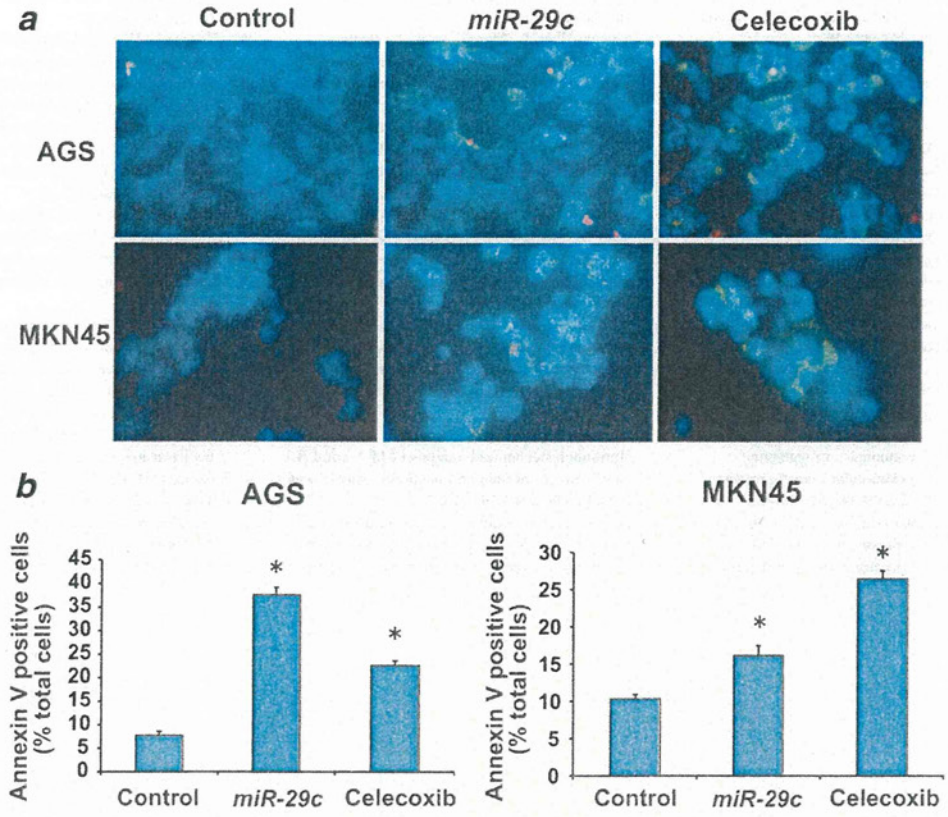

Figure 4. Celecoxib and *miR-29c* induce apoptosis in gastric cancer cells. Annexin V-FITC staining in AGS and MKN45 cells was analyzed by fluorescence microscopy (*a*) and flow cytometry (*b*). Annexin V staining (green staining on the cell surface membrane) was markedly increased in AGS and MKN45 cells 48 hr after *miR-29c* transfection and celecoxib treatment (*$p < 0.05$).

Further investigations will be needed to clarify the molecular mechanism underlying the recruitment of C/EBPα at the *miR-29c* promoter region by selective COX-2 inhibitors.

In conclusion, the tumor suppressor *miR-29c* is downregulated with overexpression of its target oncogene Mcl-1 in gastric cancers and plays important roles in cancer progression. Treatment of gastric cancer cells with the selective COX-2 inhibitor celecoxib activates *miR-29c* expression, resulting in suppression of Mcl-1 and induction of apoptosis in the cells. Administration of selective COX-2 inhibitors may have promise for the treatment of gastric cancer via restoration of *miR-29c*.

Acknowledgements

The authors thank Kana Yamada for her technical assistance.

References

1. He L, Hannon GJ. MicroRNAs: small RNAs with a big role in gene regulation. *Nat Rev Genet* 2004;5:522–31.
2. Calin GA, Croce CM. MicroRNA signatures in human cancers. *Nat Rev Cancer* 2006;6: 857–66.
3. Calin GA, Croce CM. Chromosomal rearrangements and microRNAs: a new cancer link with clinical implications. *J Clin Invest* 2007; 117:2059–66.
4. Saito Y, Liang G, Egger G, et al. Specific activation of microRNA-127 with downregulation of the proto-oncogene BCL6 by chromatin-modifying drugs in human cancer cells. *Cancer Cell* 2006;9:435–43.
5. Saito Y, Jones PA. Epigenetic activation of tumor suppressor microRNAs in human cancer cells. *Cell Cycle* 2006;5: 2220–2.
6. Saito Y, Friedman JM, Chihara Y, et al. Epigenetic therapy upregulates the tumor suppressor microRNA-126 and its host gene EGFL7 in human cancer cells. *Biochem Biophys Res Commun* 2009;379:726–31.
7. Saito Y, Suzuki H, Tsugawa H, et al. Chromatin remodeling at Alu repeats by epigenetic treatment activates silenced microRNA-512-5p with downregulation of Mcl-1 in human gastric cancer cells. *Oncogene* 2009;28:2738–44.
8. Saito Y, Suzuki H, Tsugawa H, et al. Dysfunctional gastric emptying with down-regulation of muscle-specific microRNAs in Helicobacter pylori-infected mice. *Gastroenterology* 2011;140:189–98.
9. Suzuki H, Hibi T, Marshall BJ. Helicobacter pylori: present status and future prospects in Japan. *J Gastroenterol* 2007;42:1–15.
10. Suzuki H, Iwasaki E, Hibi T. Helicobacter pylori and gastric cancer. *Gastric Cancer* 2009;12:79–87.
11. Fujishiro M. Endoscopic submucosal dissection for stomach neoplasms. *World J Gastroenterol* 2006;12:5108–12.
12. Kakushima N, Fujishiro M. Endoscopic submucosal dissection for gastrointestinal neoplasms. *World J Gastroenterol* 2008;14:2962–7.
13. Esquela-Kerscher A, Slack FJ. Oncomirs - microRNAs with a role in cancer. *Nat Rev Cancer* 2006;6:259–69.
14. Saito Y, Suzuki H, Hibi T. The role of microRNAs in gastrointestinal cancers. *J Gastroenterol* 2009;44 Suppl 19:18–22.

15. Arber N, Eagle CJ, Spicak J, et al. Celecoxib for the prevention of colorectal adenomatous polyps. *N Engl J Med* 2006;355:885–95.
16. Bertagnolli MM, Eagle CJ, Zauber AG, et al. Celecoxib for the prevention of sporadic colorectal adenomas. *N Engl J Med* 2006;355: 873–84.
17. Kuo CH, Hu HM, Tsai PY, et al. Short-term celecoxib intervention is a safe and effective chemopreventive for gastric carcinogenesis based on a Mongolian gerbil model. *World J Gastroenterol* 2009;15:4907–14.
18. Zhang LJ, Wang SY, Huo XH, et al. Anti-Helicobacter pylori therapy followed by celecoxib on progression of gastric precancerous lesions. *World J Gastroenterol* 2009;15:2731–8.
19. Mott JL, Kobayashi S, Bronk SF, et al. mir-29 regulates Mcl-1 protein expression and apoptosis. *Oncogene* 2007;26:6133–40.
20. Sengupta S, den Boon JA, Chen IH, et al. MicroRNA 29c is down-regulated in nasopharyngeal carcinomas, up-regulating mRNAs encoding extracellular matrix proteins. *Proc Natl Acad Sci USA* 2008;105:5874–8.
21. Friedman JM, Liang G, Liu CC, et al. The putative tumor suppressor microRNA-101 modulates the cancer epigenome by repressing the polycomb group protein EZH2. *Cancer Res* 2009;69:2623–9.
22. Guo Y, Chen Z, Zhang L, et al. Distinctive microRNA profiles relating to patient survival in esophageal squamous cell carcinoma. *Cancer Res* 2008;68:26–33.
23. Stamatopoulos B, Meuleman N, Haibe-Kains B, et al. microRNA-29c and microRNA-223 down-regulation has in vivo significance in chronic lymphocytic leukemia and improves disease risk stratification. *Blood* 2009;113:5237–45.
24. Mraz M, Malinova K, Kotaskova J, et al. miR-34a, miR-29c and miR-17-5p are downregulated in CLL patients with TP53 abnormalities. *Leukemia* 2009;23:1159–63.
25. Ueda T, Volinia S, Okumura H, et al. Relation between microRNA expression and progression and prognosis of gastric cancer: a microRNA expression analysis. *Lancet Oncol* 2010;11: 136–46.
26. Krajewski S, Bodrug S, Gascoyne R, et al. Immunohistochemical analysis of Mcl-1 and Bcl-2 proteins in normal and neoplastic lymph nodes. *Am J Pathol* 1994;145:515–25.
27. Wu CC, Lin JC, Yang SC, et al. Modulation of the expression of the invasion-suppressor CRMP-1 by cyclooxygenase-2 inhibition via reciprocal regulation of Sp1 and C/EBPalpha. *Mol Cancer Ther* 2008;7:1365–75.
28. Kozopas KM, Yang T, Buchan HL, et al. MCL1, a gene expressed in programmed myeloid cell differentiation, has sequence similarity to BCL2. *Proc Natl Acad Sci USA* 1993;90:3516–20.
29. Shigemasa K, Katoh O, Shiroyama Y, et al. Increased MCL-1 expression is associated with poor prognosis in ovarian carcinomas. *Jpn J Cancer Res* 2002;93:542–50.
30. Taniai M, Grambihler A, Higuchi H, et al. Mcl-1 mediates tumor necrosis factor-related apoptosis-inducing ligand resistance in human cholangiocarcinoma cells. *Cancer Res* 2004;64: 3517–24.
31. Zhou P, Qian L, Kozopas KM, et al. Mcl-1, a Bcl-2 family member, delays the death of hematopoietic cells under a variety of apoptosis-inducing conditions. *Blood* 1997;89:630–43.
32. Krajewska M, Fenoglio-Preiser CM, Krajewski S, et al. Immunohistochemical analysis of Bcl-2 family proteins in adenocarcinomas of the stomach. *Am J Pathol* 1996;149:1449–57.
33. Maeta Y, Tsujitani S, Matsumoto S, et al. Expression of Mcl-1 and p53 proteins predicts the survival of patients with T3 gastric carcinoma. *Gastric Cancer* 2004;7:78–84.

OPEN ACCESS Freely available online

PLOS | ONE

Fenton Reaction Induced Cancer in Wild Type Rats Recapitulates Genomic Alterations Observed in Human Cancer

Shinya Akatsuka[1], Yoriko Yamashita[1], Hiroki Ohara[1], Yu-Ting Liu[2], Masashi Izumiya[3], Koichiro Abe[3,4], Masako Ochiai[3], Li Jiang[1], Hirotaka Nagai[1,2], Yasumasa Okazaki[1], Hideki Murakami[5], Yoshitaka Sekido[5], Eri Arai[6], Yae Kanai[6], Okio Hino[7], Takashi Takahashi[8], Hitoshi Nakagama[3], Shinya Toyokuni[1]*

1 Departments of Pathology and Biological Responses, Nagoya University Graduate School of Medicine, Showa-ku, Nagoya, Japan, **2** Department of Pathology and Biology of Diseases, Kyoto University Graduate School of Medicine, Sakyo-ku, Kyoto, Japan, **3** Division of Cancer Development System, National Cancer Center Research Institute, Chuo-ku, Tokyo, Japan, **4** Department of Internal Medicine, Teikyo University School of Medicine, Itabashi-ku, Tokyo, Japan, **5** Division of Molecular Oncology, Aichi Cancer Center Research Institute, Chikusa-Ku, Nagoya, Japan, **6** Division of Molecular Pathology, National Cancer Center Research Institute, Chuo-ku, Tokyo, Japan, **7** Department of Pathology and Oncology, Juntendo University School of Medicine, Bunkyo-ku, Tokyo, Japan, **8** Molecular Carcinogenesis, Nagoya University Graduate School of Medicine, Showa-ku, Nagoya, Japan

Abstract

Iron overload has been associated with carcinogenesis in humans. Intraperitoneal administration of ferric nitrilotriacetate initiates a Fenton reaction in renal proximal tubules of rodents that ultimately leads to a high incidence of renal cell carcinoma (RCC) after repeated treatments. We performed high-resolution microarray comparative genomic hybridization to identify characteristics in the genomic profiles of this oxidative stress-induced rat RCCs. The results revealed extensive large-scale genomic alterations with a preference for deletions. Deletions and amplifications were numerous and sometimes fragmented, demonstrating that a Fenton reaction is a cause of such genomic alterations *in vivo*. Frequency plotting indicated that two of the most commonly altered loci corresponded to a *Cdkn2a/2b* deletion and a *Met* amplification. Tumor sizes were proportionally associated with *Met* expression and/or amplification, and clustering analysis confirmed our results. Furthermore, we developed a procedure to compare whole genomic patterns of the copy number alterations among different species based on chromosomal syntenic relationship. Patterns of the rat RCCs showed the strongest similarity to the human RCCs among five types of human cancers, followed by human malignant mesothelioma, an iron overload-associated cancer. Therefore, an iron-dependent Fenton chemical reaction causes large-scale genomic alterations during carcinogenesis, which may result in distinct genomic profiles. Based on the characteristics of extensive genome alterations in human cancer, our results suggest that this chemical reaction may play a major role during human carcinogenesis.

Citation: Akatsuka S, Yamashita Y, Ohara H, Liu Y-T, Izumiya M, et al. (2012) Fenton Reaction Induced Cancer in Wild Type Rats Recapitulates Genomic Alterations Observed in Human Cancer. PLoS ONE 7(8): e43403. doi:10.1371/journal.pone.0043403

Editor: Kamaleshwar Singh, Texas Tech University, United States of America

Received March 2, 2012; **Accepted** July 19, 2012; **Published** August 29, 2012

Copyright: © 2012 Akatsuka et al. This is an open-access article distributed under the terms of the Creative Commons Attribution License, which permits unrestricted use, distribution, and reproduction in any medium, provided the original author and source are credited.

Funding: This study was supported by Princess Takamatsu Cancer Research Fund (10-24213); a Grant-in-Aid for Cancer Research from the Ministry of Health, Labour and Welfare of Japan; and a Grant-in Aid from the Ministry of Education, Culture, Sports, Science and Technology of Japan. The funders had no role in study design, data collection and analysis, decision to publish, or preparation of the manuscript.

Competing Interests: The authors have declared that no competing interests exist.

* E-mail: toyokuni@med.nagoya-u.ac.jp

Introduction

Cancer is a disease of accumulated genomic alterations, presumably caused by a systematic process during cellular injury and repair. Causative agents for carcinogenesis are numerous including γ-radiation, ultraviolet radiation, inflammation, chemicals and iron overload [1]. Genomic data of a variety of human cancers is currently analyzed either with array-based comparative genomic hybridization (CGH) [2] or next-generation sequencing [3,4]. These projects are performed to find causative gene mutations that will lead to identifying novel chemicals or antibodies directed for the interactions of responsible signaling molecules. These efforts are expected to result in developments of effective drugs. However, cancer prevention in daily life is as important as its therapy.

In the present study, we sought to resolve roles of iron-mediated oxidative stress during carcinogenesis using array-based CGH. Oxidative stress is constitutively caused by the metabolism of molecular oxygen [5], but is mainly regulated by various antioxidant systems. However, in a variety of pathological conditions, oxidative stress loads exceed the antioxidant capacity [6]. Iron is the most abundant heavy metal in mammals, such as rodents and humans. Whereas iron is essential for oxygen transport as a component of hemoglobin, excess iron has been associated with carcinogenesis [7,8], presumably through a Fenton reaction [9]. Ionic forms of iron are barely soluble at a neutral pH, but ferric nitrilotriacetate (Fe-NTA), an iron chelate, is soluble at pH 7.4 and is an efficient catalytic agent for the Fenton reaction [10]. In the 1980s, our group established that repeated intraperitoneal administrations of Fe-NTA induce a high incidence of renal cell carcinoma (RCC) in rodents [11,12]. Later, we

showed that the renal injury occurs through a Fenton reaction with a variety of hydroxyl radical-mediated chemical products, such as 8-hydroxy-2′-deoxyguanosine [13,14] and 4-hydroxy-nonenal [15,16]. It is established that an iron overload in many pathological conditions is associated with the presence of catalytic iron [17,18].

Accordingly, by evaluating whole genome of RCCs, we could find a general principle for the genomic alterations under oxidatively-stressed conditions. We reported a *Cdkn2a/2b* deletion using microsatellite analysis in this model [19]. In this study, we evaluated the whole genome of Fe-NTA-induced rat RCCs and their cell lines using array-based CGHs. Furthermore, we transformed the data into a human genome through chromosomal syntenic relationship and analyzed the association.

Results

Genome-wide Views of DNA Copy Number Alterations in Fe-NTA-induced Rat RCCs

Fifteen rat RCC DNA samples, which included 13 primary tumor samples and 2 cell line samples, were hybridized on Agilent oligonucleotide microarrays for CGH with 181,978 genomic loci (GEO accession: GSE36101). Comparing different array-based CGH profiles in a quantitative manner is difficult. A shift in the mean copy number is caused by polyploidy and the contamination of normal cells. Therefore, we have developed a statistical method that considers these factors to estimate the chromosomal copy number (**Methods S1**). In this paper, array-based CGH profile data analyses are based on the estimated copy numbers using this method.

Array-based CGH profiling revealed that genomes of the Fe-NTA-induced rat RCCs are often complex and have many extensive chromosomal alterations (**Figs. 1A and S1**). A whole genome frequency analysis with 15 samples identified recurrent regions of a copy number aberration in the Fe-NTA-induced RCCs (**Fig. 1B**). Copy number aberrations were determined based on the distribution of the log2 ratio values that were recalculated with the estimated copy number for a set of 13 primary tumors and 2 cell lines (**Fig. S2**). In this distribution, the thresholds that represented gain and loss were chosen at ± 0.377. A threshold representing amplification was chosen at +0.811 whereas a homozygous deletion (complete loss) was assigned to the position at which the copy number was estimated as 0. The most characteristic global feature uncovered by the frequency analysis was a predisposition to lose an extensively wide region of chromosomes, especially for chromosomes 3, 5, 6, 8, 9, 14, 15, 17 and 20. The second feature was a frequent amplification over a long pericentromeric region in chromosome 4.

Frequent Chromosomal Loss in Rat Chromosome 5 and Homozygous Deletion at the *Cdkn2a/2b* Locus

Chromosome 5 underwent an extensive loss in copy number, not less than that in other chromosomes (e.g., chromosomes 6, 8 and 20) (**Fig. 1B**). As it relates to extensive loss, homozygous deletions were most frequently observed at the *Cdkn2a/2b* locus on chromosome 5 (**Fig. 2A**). This commonly deleted region included two loci (*Cdkn2a* and *Cdkn2b*) for three distinct tumor suppressor genes (*p16* and *p19* in *Cdkn2a*; *p15* in *Cdkn2b*) (**Fig. 2B**). Shutdown of *p16/p19* and *p15* mRNA expression was confirmed in the samples that contained a homozygous deletion at the *Cdkn2a/2b* locus (**Figs. 2C and 2D**). In samples with a hemizygous deletion at the *Cdkn2a* locus (i.e., FB32-4, FB28-7), *p16* and *p19* expressions were downregulated, presumably because the promoter regions of the remaining alleles were methylated. However, some of the samples with either a hemizygous or no deletion (e.g., FB14-3; BF51-1; FB14-6; FB30-5 and FB33-7) showed a marked overexpression of *p16* and *p19*.

Frequent Amplifications Over the Pericentromeric Region of Chromosome 4 and Amplification at the *Met* Locus

Over a long portion of the pericentromeric region in chromosome 4, frequent copy number gain and amplification were observed (**Fig. 1B**). Genomic amplification and gene expression in the corresponding areas of chromosome 4 were mostly proportional (**Fig. S3**). A bar plot of the amplified region along the pericentromeric region in chromosome 4 revealed that *Met* oncogene resides in the most common overlapping genomic section (**Fig. 3A**). The most overlapping section with a length of approximately 222 kb consisted of an amplified region in 11/15 samples and contained only one RefSeq-curated gene (*Met*) (**Fig. 3B**). A greater than 5-fold increase in *Met* mRNA expression was observed in 6 samples among the 9 tumors that contained a genomic amplification of *Met* (**Fig. 3C**).

Collectively, regarding chromosomal aberrations at these two cancer-related loci, every examined carcinoma including the two cell lines contained either the *Met* amplification or the *Cdkn2a/2b* deletion (**Table 1, Figs. 2B and 3B**). Other common genetic alterations are summarized in **Table S1** (20 deleted genes, common in 2–4 RCC tumors) and **Table S2** (340 amplified genes, common in 2–9 RCC tumors). Among those *Zbtb38* amplification was confirmed for overexpression (**Fig. S4**).

Tumor Size of Fe-NTA-induced RCCs is Regulated by Genetic Features

We examined the associations between genetic alterations and various RCC traits including those summarized in **Table 1**. Among all of the relationships examined, *Met* expression and tumor size were proportionally associated (**Fig. 4A**). Furthermore, a hierarchical clustering of tumors based on whole patterns of chromosomal changes revealed that a group of large tumors (i.e., FB7-7, FB30-5 and FB33-7) corresponded to a distinct cluster (**Fig. 4B**). Therefore, a tumor trait, size at the time the tumor was clinically overt, was associated with the entire array-based CGH profiles.

Comparison of Copy Number Alteration Profiles in Cancer Genomes Between Rats and Humans

To determine the general principle of large-scale genomic changes in cancer across mammalian species, we compared cancer genomes of rats and humans as a whole spectrum of chromosomal alterations. First, we transformed the rat array-based CGH profiles onto human chromosomes according to a synteny between the two species. Thereafter, we compared the whole patterns based on estimated copy numbers using multidimensional data analysis methods. We found that Fe-NTA-induced rat RCC was most similar to human RCCs, followed by human malignant mesothelioma (**Figs. 5A and 5B**).

Discussion

In this study, we report for the first time analyses of the entire data from array-based CGH applied to a Fenton chemistry-induced carcinogenesis in a rat kidney model [20]. We found that oxidative stress causes extensive genomic alterations in the induced cancer genome at chromosomal level (**Fig. 1A**). It is well known that a majority of human malignant solid tumors possess gains or losses in numerous chromosomes [21,22], and amplification can

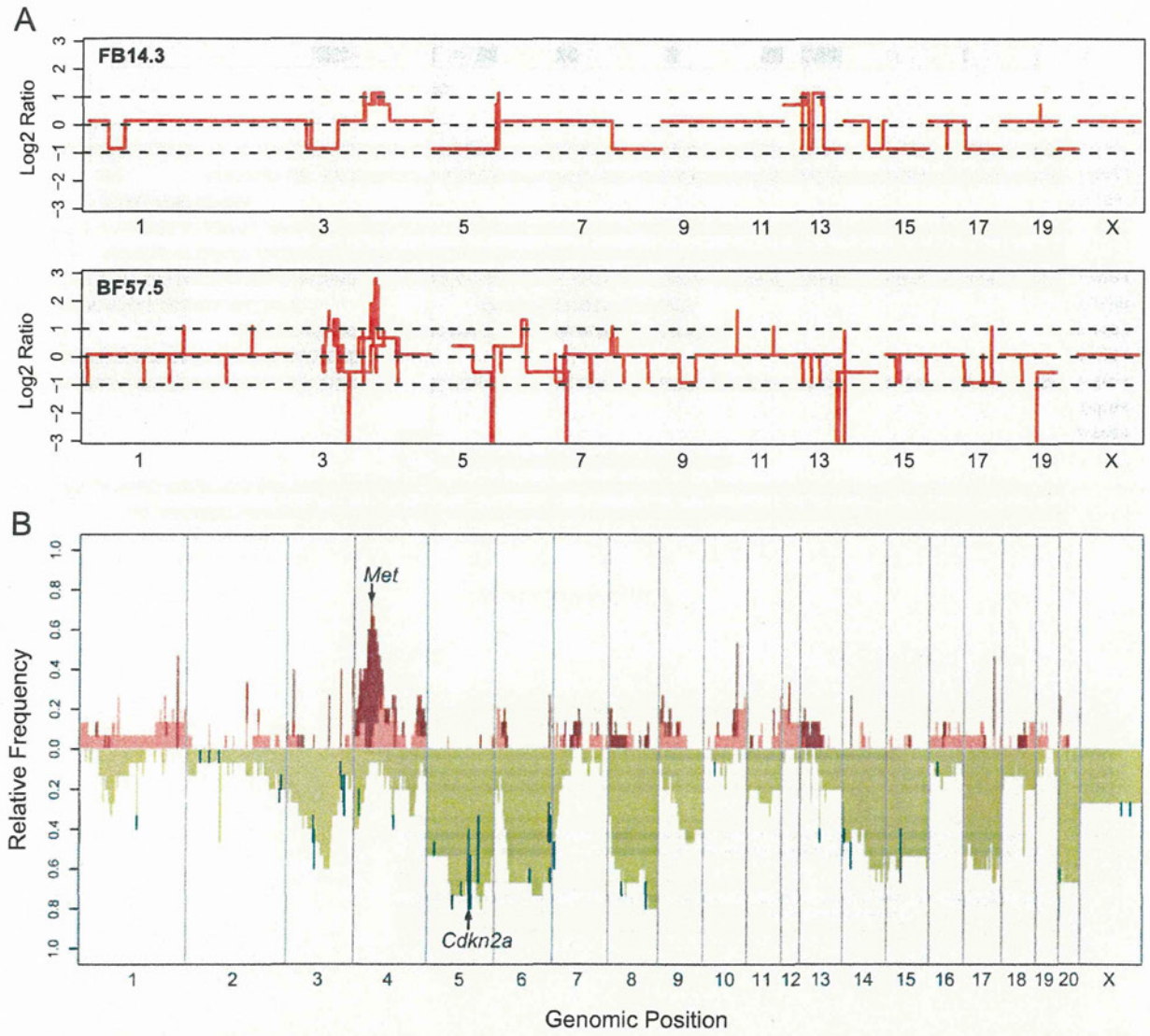

Figure 1. Genome-wide views of DNA copy number alterations in Fe-NTA induced rat renal cell carcinomas (RCCs). (A) Representative array-based CGH profiles from two RCC tumors. The red lines show log2 ratios of the estimated copy number over the inferred cancer ploidy versus the genomic position for all of the CGH microarray probes. (B) Frequency distribution of copy number aberrations across the whole rat genome. The relative frequencies of amplification (dark red), gain (tomato), loss (green yellow) and homozygous deletion (dark green) within 13 RCC tumors and two RCC cell lines are plotted at each genomic position. Two cancer-related loci, *Met* and *Cdkn2a*, which were most frequently affected by copy number aberration are indicated by the arrows.
doi:10.1371/journal.pone.0043403.g001

be a suitable target for cancer chemotherapy. During the carcinogenic process of such tumors, chromosomal instability is thought to contribute as a driving factor [23]. Among wild-type rodent carcinogenesis models, however, few models report using primary tumor samples extensive genetic alterations because of chromosomal instability [24,25]. Radiation-induced murine malignant lymphoma [26] and murine lung adenocarcinoma induced by 4-(methylnitrosamino)-1-(3-pyridyl)-1-butanone, a carcinogen present in tobacco smoke [27], revealed slightly more gross chromosomal aberrations than the corresponding spontaneous tumors, albeit the low resolution in the report (bacterial artificial chromosome [BAC] array of ~6,500). The facts that control rats exhibit no RCCs [11,12] and Fe-NTA-induced rat RCC model exhibits an equivalence to human cancers in genomic alterations at chromosomal level strongly support the idea that this carcinogenesis model mimics an actual carcinogenic process in those humans who lack strong cancer susceptibility traits.

Conversely, mice with multiple genetically-engineered cancer-associated genes show genetic alteration of this kind [28]. We think that those experiments correspond to an established mutator phenotype [29] and, thus, to the carcinogenic process in humans who have strong cancer susceptibility traits such as Li-Fraumeni syndrome (*p53*) [30] or melanoma kindreds (*p16*) [31]. As a hereditary rat RCC model, we also analyzed the RCCs of Eker rats, which do not show aggressive characteristics, such as metastasis [32,33,34]. We observed that these RCCs showed null

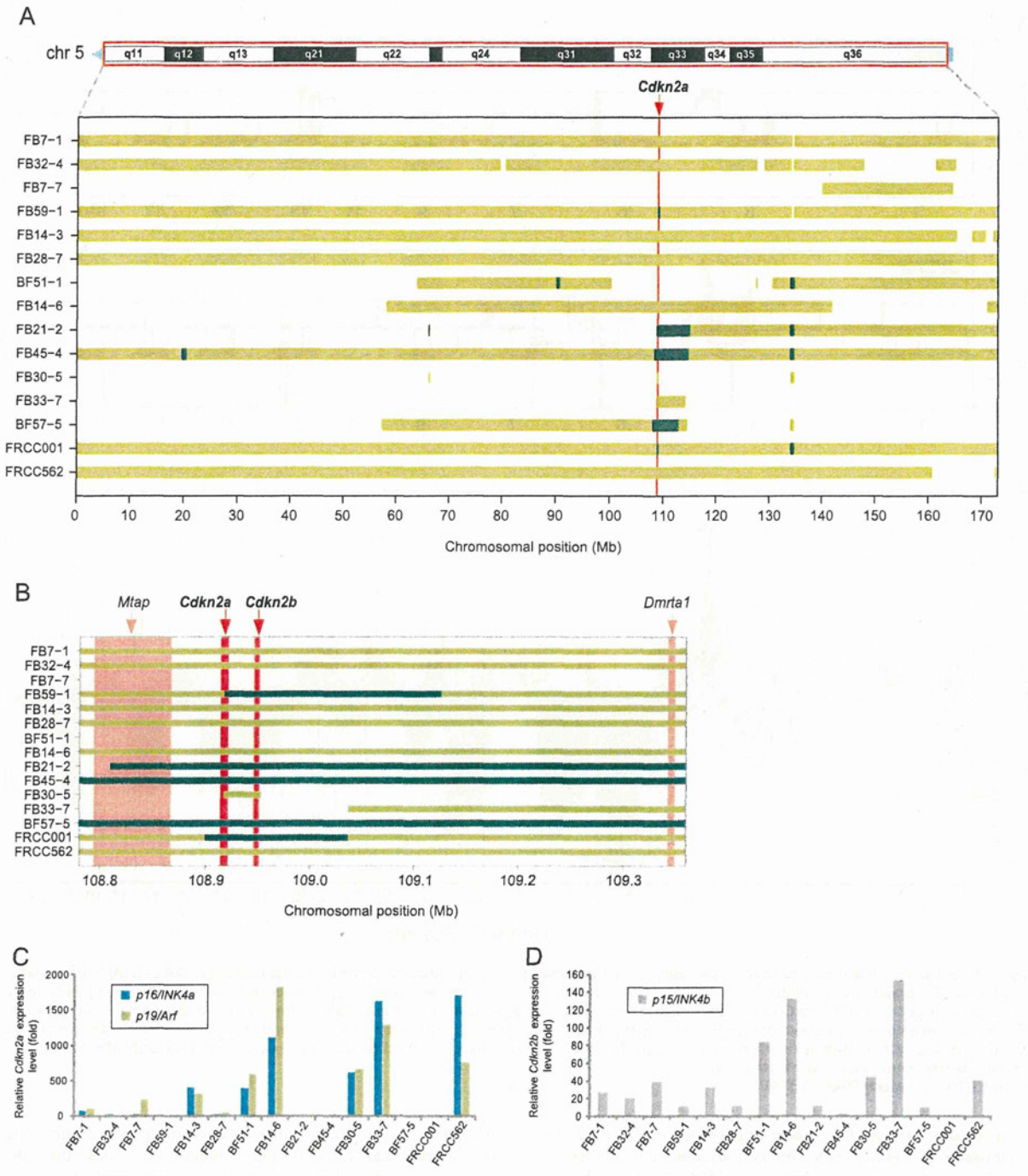

Figure 2. Frequent extensive chromosomal losses in rat chromosome 5, and homozygous deletions at the region including the *Cdkn2a* and *Cdkn2b* loci. (A) The bar chart represents the regions of chromosomal loss (green yellow) and homozygous deletion (dark green) along chromosome 5 for 13 RCC tumors and two RCC cell lines. The vertical red line on the background indicates the position of the *Cdkn2a* locus. (B) Magnified view of the bar chart centered on the *Cdkn2a/2b* loci. The genomic regions of all of the RefSeq genes included in the displayed range of the chromosome are depicted as vertical bars on the background. (C) Expression analysis of *Cdkn2a* ($p16^{Ink4a}$ and $p19^{Arf}$) for 13 RCC tumors and two RCC cell lines, using real-time PCR with specific primer pairs for each different transcript. The values on the *y*-axis indicate relative mRNA expression level compared to an average of those in normal kidneys of three control rats. (D) Expression analysis of *Cdkn2b* ($p15^{Ink4b}$) for 13 RCC tumors and two RCC cell lines by real-time PCR. The values on the *y*-axis indicate relative mRNA expression level compared to an average of those in normal kidneys of three control rats.

doi:10.1371/journal.pone.0043403.g002

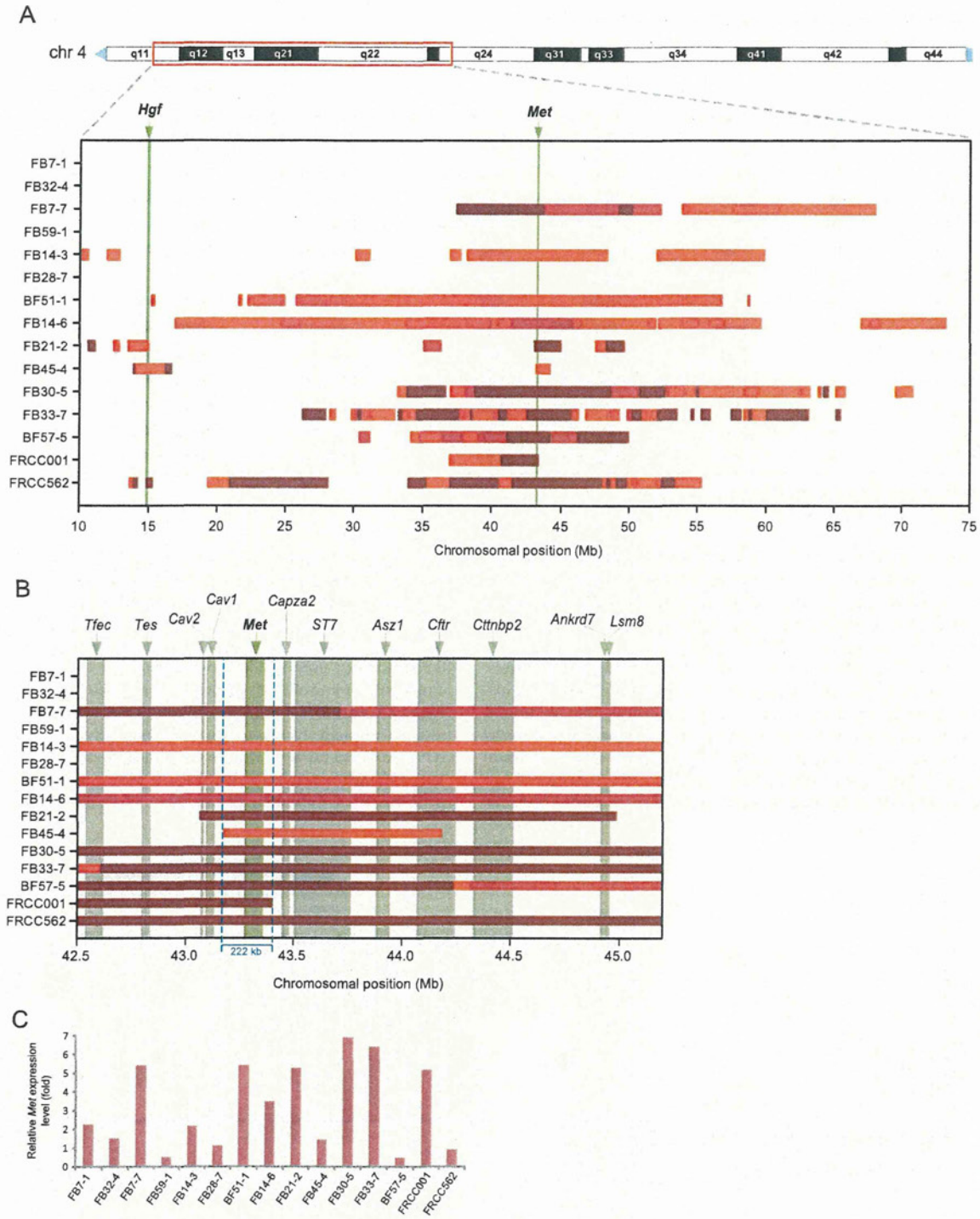

Figure 3. Frequent wide-ranging amplifications over a long pericentromeric region of chromosome 4 with the *Met* oncogene residing in the most overlapping section. (A) The bar chart represents the amplification regions along a 65 Mb pericentrometic region of chromosome 4 for 13 RCC tumors and two RCC cell lines. Four grades of amplification are indicated by bar color gradation; the darker the red, the larger the amplitude. (B) A magnified view of the bar chart above shows the vicinity of the most overlapping region. The genomic regions of all of the RefSeq genes included in the displayed range of the chromosome are depicted as vertical bars in the background. (C) Expression analysis of *Met* for 13 RCC tumors and two RCC cell lines by real-time PCR. The values on the *y*-axis indicate relative mRNA expression level compared to an average of those in normal kidneys of three control rats.
doi:10.1371/journal.pone.0043403.g003